Supporting Information for

Mitigation mechanism of membrane fouling in MnFeOx functionalized ceramic membrane catalyzed ozonation process for treating natural surface water

Hui Guo [1,2,†], Yanxiao Chi [1,†], Yifan Jia[1], Manman Li [6], Yuxuan Yang [1],

Haiyong Yao [1,2], Kunlun Yang [1,*] , Zengshuai Zhang [1], Xueli Ren [1], Peng Gu [1], Hengfeng Miao [1,3,4,5,*]

1 School of Environmental and Civil Engineering, Jiangnan University, Wuxi 214122, P.R. China;

2 Zhejiang Juneng Environmental Co., Ltd., Tongxiang 314599, Zhejiang, China;

3 Jiangsu Key Laboratory of Anaerobic Biotechnology, Jiangnan University, Wuxi 214122, PR China;

4 Jiangsu Engineering Laboratory of Biomass Energy and Carbon Reduction Technology, Jiangnan University, Wuxi 214122, PR China

5 Jiangsu Collaborative Innovation Center of Technology and Material of Water Treatment，Suzhou University of Science and Technology, Suzhou 215009, PR China

6 Academy of Intelligence Environment Protection and Monitoring Technology, Co., Ltd., Wuxi 214000, PR China

*Corresponding authors:

Kunlun Yang, e-mail: yangkunlun@jiangnan.edu.cn

Hengfeng Miao, e-mail: hfmiao@jiangnan.edu.cn

Supplemental data caption

Text S1. Effectiveness of the combined process on the removal of TMP.

Table S1. The BET tests of (a) the original ceramic membrane and (b) the Mn-Fe-CM.

Figure S1. Characterizations of CMs (a) SEM image of pristine CM, (b) and (c) SEM images of Mn-CM and Fe-CM, (d) and (e) the surface of Mn-Fe-CM, (f) the cross section of Mn-Fe-CM, (g) and (h) TEM of Mn/FeOx, (i) the cyclic voltammetry of CMs.

Figure S2. (a) The EDS and (b) XRD image of modified-ceramic membrane.

Figure S3. XPS spectra of (a) The full survey spectrum, (b) O 1 s spectrum, (c) and (e) Mn 2p spectrum of Mn-Fe-CM before and after catalytic ozonation, (d) and (f) Fe 2p spectrum of Mn-Fe-CM before and after catalytic ozonation.

Figure S4. The concentration changes of TMP in the effluent of different processes.

Figure S5. The water contact angle of (a) the original ceramic membrane and (b) the Mn-Fe-CM.

Figure S6. N_2 Adsorption-Desorption Isotherm of (a) original ceramic membrane and (b) the Mn-Fe-CM. And the pore diameter distribution of (c) original ceramic membrane and (d) the Mn-Fe-CM.

Figure S7. Effect of radical scavengers on the degradation of TMP.

Figure S8. EPR spectra in different systems: (a) DMPO-·OH, (b) TEMP-$^1O_2$.

Text S1: Effectiveness of the combined process on the removal of TMP.

Figure S4. examines the removal of TMP added to surface water by the combined process. The removal of TMP in the effluent of the conventional process was 52.0%, part of which may be adsorbed on the coagulant and quartz sand with the coagulation-sedimentation-sand filtration process, and part may be degraded by microorganisms present in the raw water; the removal of TMP in the effluent of the conventional process combined with O_3 increased by 30%. It can be seen that O_3 is efficient for organic removal, and the removal rate of TMP in O_3/Mn-Fe-CM effluent reached 95.6%, so coagulation-precipitation-sand filtration pretreatment of raw water can effectively improve the removal effect of organic matter. [1]

Table S1. The BET tests of (a) the original ceramic membrane and (b) the Mn-Fe-CM.

Sample type	BET surface area (m^2/g)	Total pore volume (cm^3/g)	Average pore diameter (nm)
Original CM	1.7401	0.0095672	1.74
Fe-Mn-CM	1.6353	0.0096766	1.74

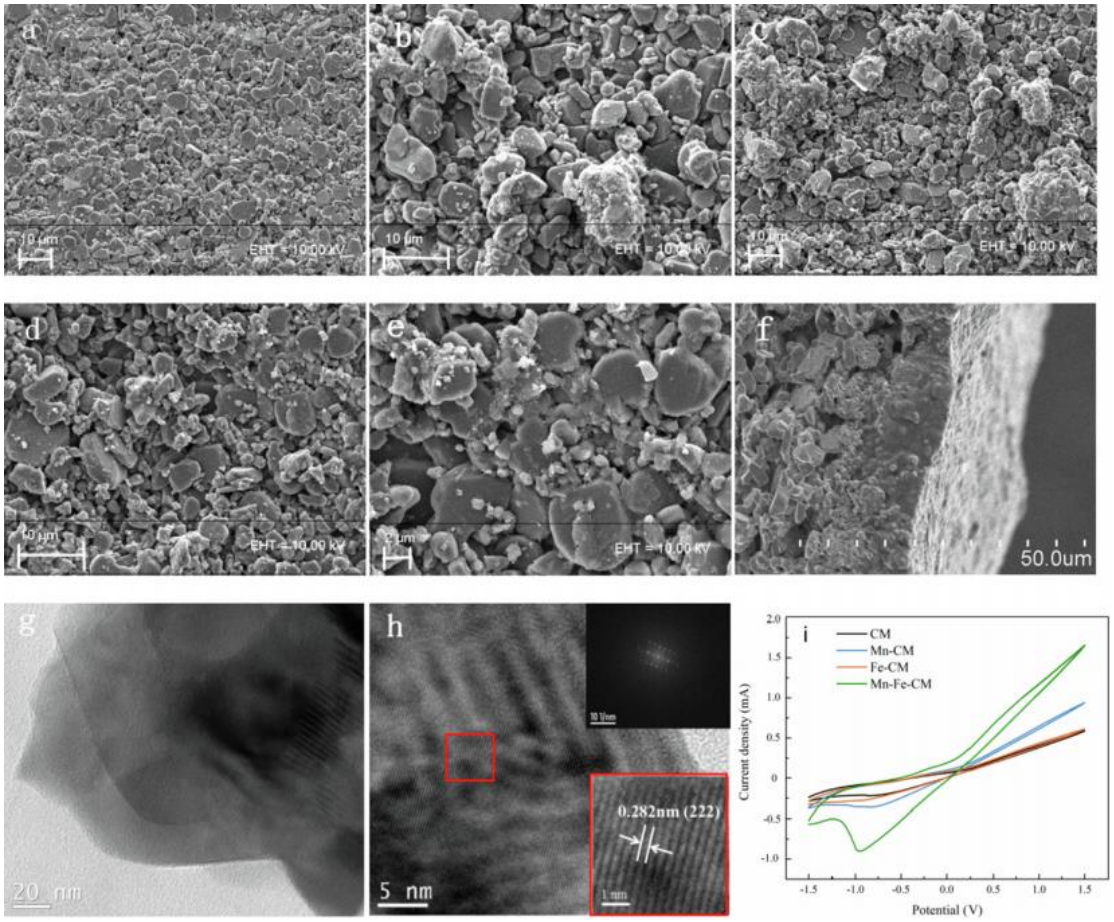

Figure S1. Characterizations of CMs (a) SEM image of pristine CM, (b) and (c) SEM images of Mn-CM and Fe-CM, (d) and (e) the surface of Mn-Fe-CM, (f) the cross section of Mn-Fe-CM, (g) and (h) TEM of Mn/FeOx, (i) the cyclic voltammetry of CMs.

In the SEM Fig. a-f, the surface size of the modified film is uniform and the roughness is reduced, and some of the membrane pores can still be seen distributed on the surface of the film, it is presumed that the addition of appropriate amount of iron can reduce the particle size of MnOx and make its dispersion better.

In the TEM Fig. g-h, it shows that Mn/FeOx has a layered structure and most of the nanosheets are close to hexagonal shape, and it is presumed that the surface loading composition of Mn-Fe-CM film is $FeMnO_3$.

As shown in Fig. i, there are almost no obvious redox peaks on CM and Fe-CM, and there are weak currents on Mn-CM, while there are obvious redox currents on Mn-Fe-CM, indicating that Mn-Fe-CM possesses a strong catalytic oxidation ability. [1]

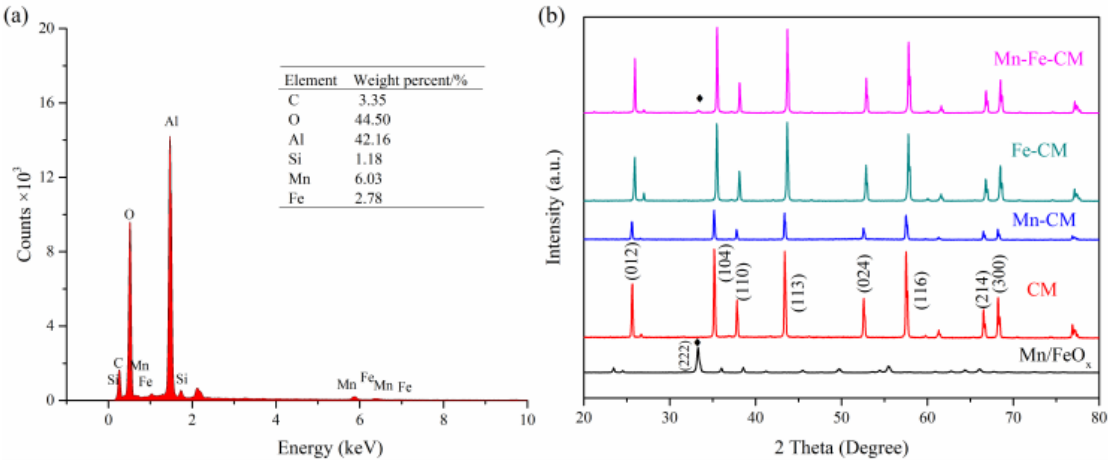

Figure S2. (a) The EDS and (b) XRD image of modified-ceramic membrane

The EDS results showed that the surface of the ceramic film was mainly composed of Al and O and was successfully loaded with Fe and Mn on Mn-Fe-CM (Fe: 2.78%, Mn: 6.03%).

The XRD pattern of Mn-Fe-CM shows that the crystalline peak of Mn/FeOx is detected, and the results are consistent with those in TEM, which further indicates that the surface loading layer composition of Mn-Fe-CM is mainly $FeMnO_3$. [1]

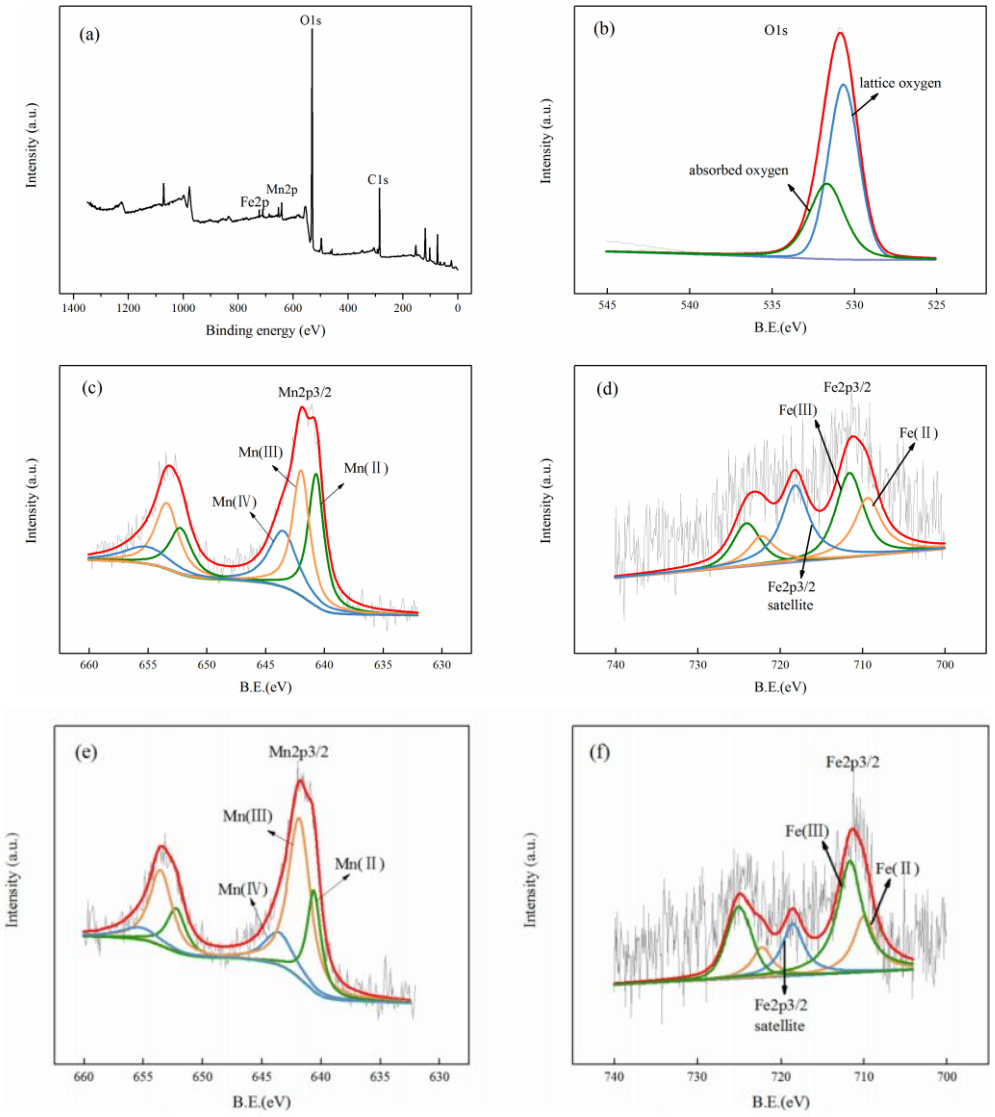

Figure S3. XPS spectra of (a) The full survey spectrum, (b) O 1 s spectrum, (c) and (e) Mn 2p spectrum of Mn-Fe-CM before and after catalytic ozonation, (d) and (f) Fe 2p spectrum of Mn-Fe-CM before and after catalytic ozonation.

XPS characterization of the surface of Mn-Fe-CM before and after the catalytic reaction showed that Fe(II)/Fe(III) and Mn(III)/Mn(IV) underwent electron transfer and redox reactions in O_3 solution, and it is presumed that Fe(III), Mn(III) and Mn(IV) participated in the catalytic process of O_3 as the catalytic active sites of Mn-Fe-CM, which also indicates that the prepared Mn-Fe-surface loading layer has good catalytic activity [1].

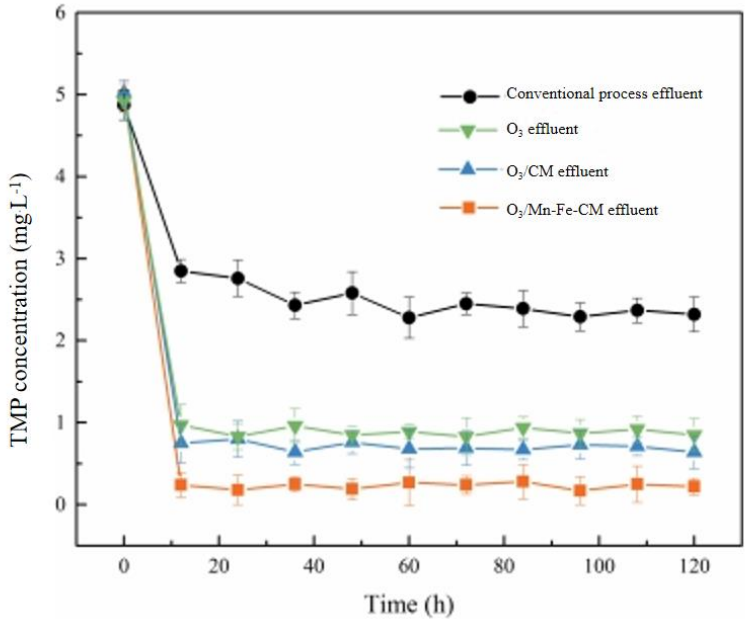

Figure S4. The concentration changes of TMP in the effluent of different processes

Coagulation-sedimentation-sand filtration pretreatment of raw water can effectively improve the removal effect of organic matter [1].

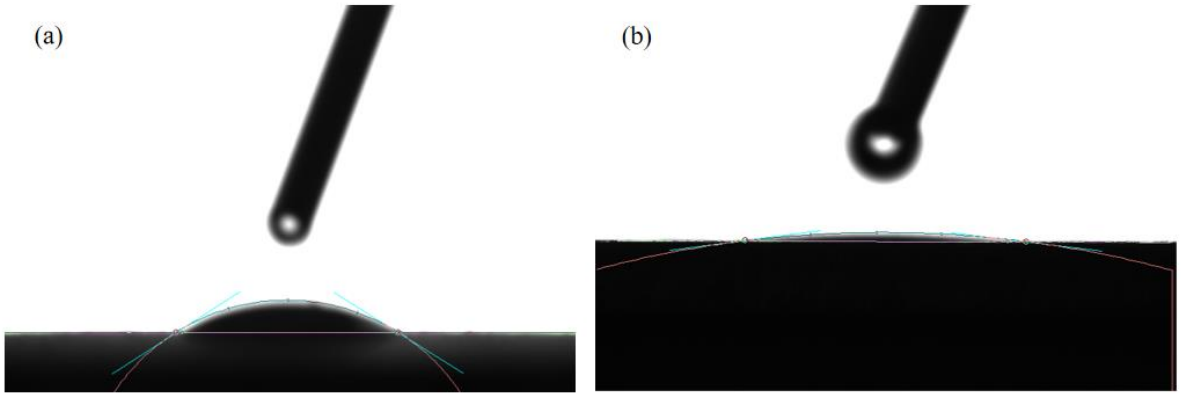

Figure S5. The water contact angle of (a) the original ceramic membrane and (b) the Mn-Fe-CM.

The water contact angle decreased from 35.1° to 8.3° after loading FeMnOx. It indicates that the loaded Mn-Fe-CM has better hydrophilic properties.

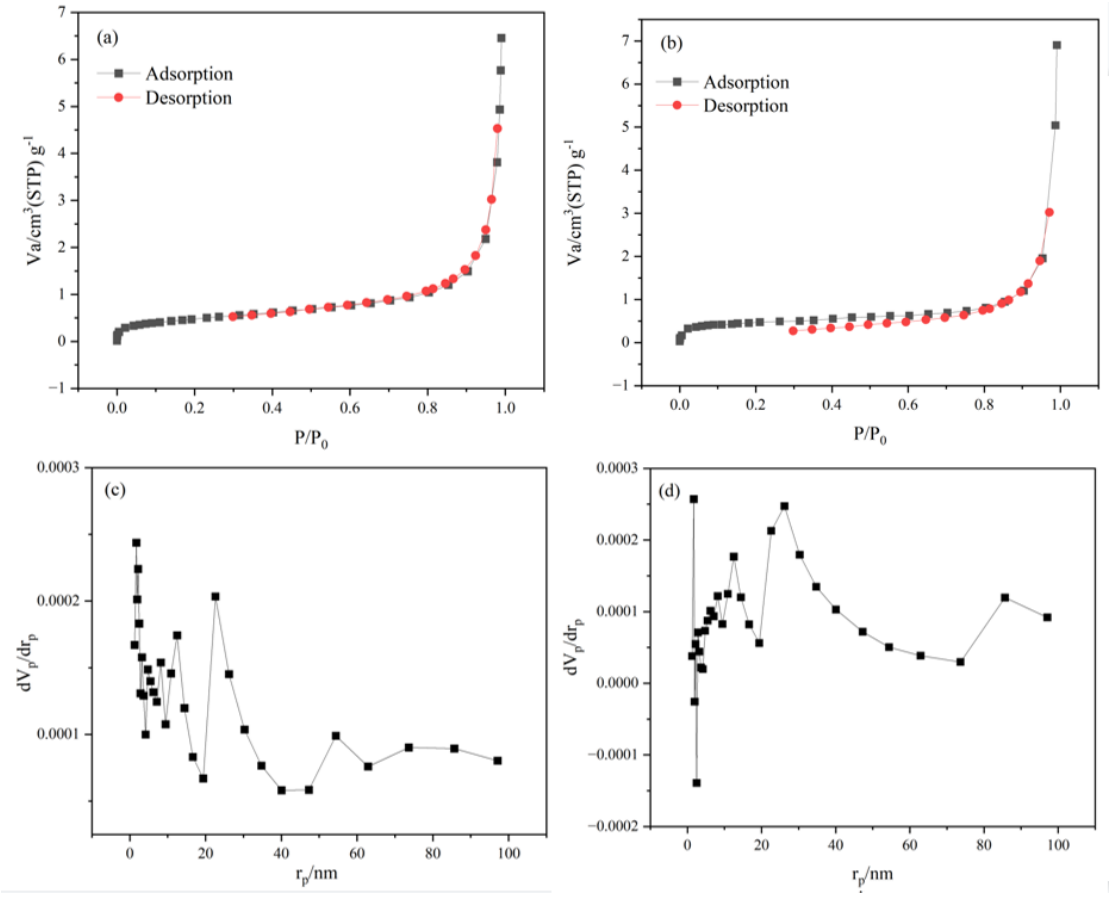

Figure S6. N_2 Adsorption-Desorption Isotherm of (a) original ceramic membrane and (b) the Mn-Fe-CM. And the pore diameter distribution of (c) original ceramic membrane and (d) the Mn-Fe-CM.

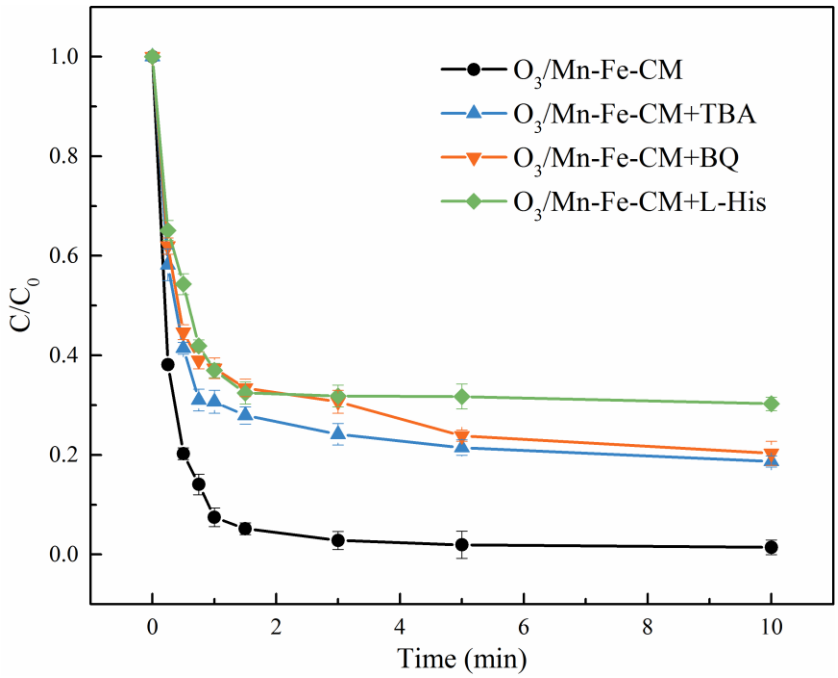

Figure S7. Effect of radical scavengers on the degradation of TMP

It is presumed that the reactive oxygen species involved in the degradation process of TMP are mainly $^1O_2$ and ·OH [1]. Besides, the TBA is Tert-Butanol; the BQ is p-Benzoquinone dioxime ; the L-His is L-Histidine.

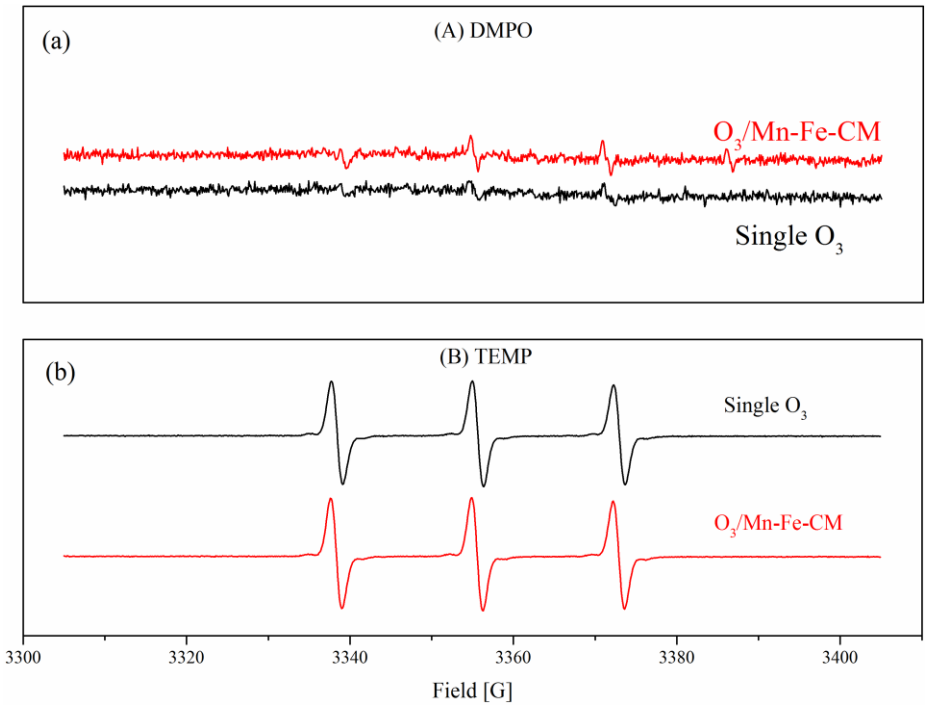

Figure S8. EPR spectra in different systems: (a) DMPO-·OH, (b) TEMP-$^1O_2$

From the results, ·OH was produced in both O_3 and O_3/Mn-Fe-CM systems, and the DMPO-·OH signal intensity was stronger in the O_3/Mn-Fe-CM system than in the O_3 system, indicating that more ·OH was produced in the O_3/Mn-Fe-CM system [1].

References

1. Li, M.; Yang, K.; Huang, X.; Liu, S.; Jia, Y.; Gu, P.; Miao, H. Efficient degradation of trimethoprim by catalytic ozonation coupled with Mn/FeOx-functionalized ceramic membrane: Synergic catalytic effect and enhanced anti-fouling performance. J *Colloid Interface Sci* **2022**, 616:440-452, doi:10.1016/j.jcis.2022.02.061